A reaction-diffusion-chemotactic biocontrol model

Asymptotics and numerical simulations

Ramón G. Plaza

Institute of Applied Mathematics (IIMAS),
National Autonomous University of Mexico (UNAM)

Collaborators:

- C. Málaga *(Physics Dept., UNAM)*
- A. Minzoni *(IIMAS, UNAM)*
- C. Simeoni *(Univ. of L'Aquila, Italy)*

Sponsors:

- MIUR (Italy) Ministero dell'Istruzione, dell'Università e della Ricerca
- CONACyT (Mexico) CONACYT

1. An experiment
2. Modeling
3. Asymptotic analysis
4. Numerical simulations

An experiment

M. SWAIN, R. RAY (2009), *Microbiol. Res.* **164.**

- Beneficial activities (biocontrol) of *Bacillus subtilis* in the presence of phytopathogenic microflora, such as *Fusarium oxysporum*
- Experiment: uniform concentration of *F. oxysporum* in a Petri dish was inoculated with *B. subtilis*
- Inhibition of the in vitro growth of the fungus
- Emergence of isolated patterns or strains free of fungus near the places where the bacteria was applied
- Patterns occur only after 24 hrs. of inoculation
- Patterns stably persist for more than six days (144 hrs.)

An experiment

M. SWAIN, R. RAY (2009), *Microbiol. Res.* **164.**

- Beneficial activities (biocontrol) of *Bacillus subtilis* in the presence of phytopathogenic microflora, such as *Fusarium oxysporum*
- Experiment: uniform concentration of *F. oxysporum* in a Petri dish was inoculated with *B. subtilis*
- Inhibition of the in vitro growth of the fungus
- Emergence of isolated patterns or strains free of fungus near the places where the bacteria was applied
- Patterns occur only after 24 hrs. of inoculation
- Patterns stably persist for more than six days (144 hrs.)

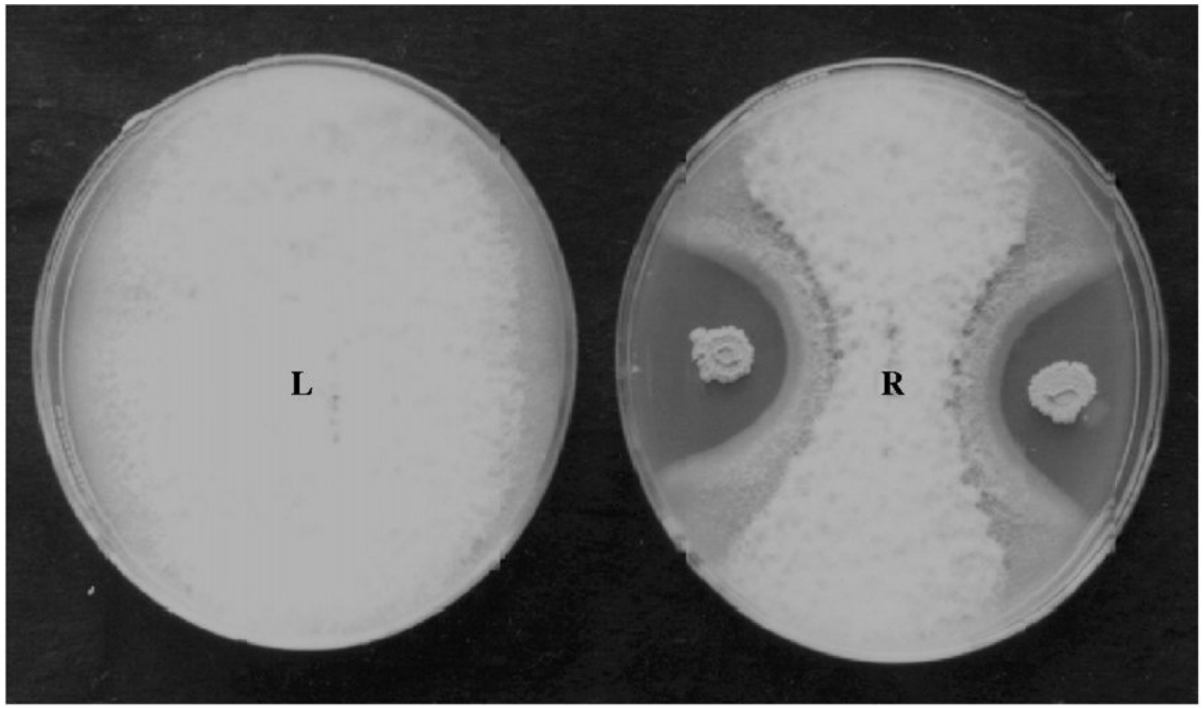

Figure: Antagonistic activity of *B. subtilis* against *F. oxysporum*. Left: control (only *F. oxysporum*); right: *B. subtilis* + *F. oxysporum*. Taken from Swain, Ray (2009), *Microbiol. Res.* vol. 164. Courtesy of Elsevier GmbH.

Questions:

- How can we model the underlying dynamics?
- What is the mechanism of triggering of fungal supression?
- Is this a chemotactic process? (KELLER, SEGEL (1970) *J. Theor. Biol.*)
- Does the system reach stable/“metastable” states?

1 An experiment

2 Modeling

3 Asymptotic analysis

4 Numerical simulations

Modeling

Facts:

- There are no reliable measurements of diffusion coefficients for the fungus.
- Zoospore chemotaxis occur in nature: ISLAM, TAHARA (2001) *Biosci. Biotechnol. Biochem.* 65.
- *Negative* zoospore chemotaxis is well-documented: ALLEN, HARVEY (1974) *J. Gen. Microbiol.* 84; CAMERON, CARLILE (1980) *J. Gen. Microbiol.* 120.
- *B. subtilis* produces anti-fungal metabolites (known as *mycosubtilin*) against *F. oxysporum*: LECLÉRE et al. (2005) *Appl. Environ. Microbiol.* 71; Nagórska et al. (2007) *Acta Biochim. Pol.* 54; LECLÉRE et al. (2006) *Arch. Microbiol.* 186.

Assumptions:

- The fungal supression mechanism is chemotactic, via the metabolite agent produced by the bacteria (chemo-repellent)
- Species diffuse and react with logistic growth with threshold
- Chemical reacts and diffuses with simple production/decay terms
- Following cell-kinetic models (e.g. HILLEN, PAINTER (2009) *J. Math. Biol.* 58) we assume small cell/zoospore diffusivity regime
- The model is not predictive; intends to understand the underlying dynamics

Assumptions:

- The fungal supression mechanism is chemotactic, via the metabolite agent produced by the bacteria (chemo-repellent)
- Species diffuse and react with logistic growth with threshold
- Chemical reacts and diffuses with simple production/decay terms
- Following cell-kinetic models (e.g. HILLEN, PAINTER (2009) *J. Math. Biol.* 58) we assume small cell/zoospore diffusivity regime
- The model is not predictive; intends to understand the underlying dynamics

Assumptions:

- The fungal supression mechanism is chemotactic, via the metabolite agent produced by the bacteria (chemo-repellent)
- Species diffuse and react with logistic growth with threshold
- Chemical reacts and diffuses with simple production/decay terms
- Following cell-kinetic models (e.g. HILLEN, PAINTER (2009) *J. Math. Biol.* 58) we assume small cell/zoospore diffusivity regime
- The model is not predictive; intends to understand the underlying dynamics

Assumptions:

- The fungal supression mechanism is chemotactic, via the metabolite agent produced by the bacteria (chemo-repellent)
- Species diffuse and react with logistic growth with threshold
- Chemical reacts and diffuses with simple production/decay terms
- Following cell-kinetic models (e.g. HILLEN, PAINTER (2009) *J. Math. Biol.* 58) we assume small cell/zoospore diffusivity regime
- The model is not predictive; intends to understand the underlying dynamics

Assumptions:

- The fungal supression mechanism is chemotactic, via the metabolite agent produced by the bacteria (chemo-repellent)
- Species diffuse and react with logistic growth with threshold
- Chemical reacts and diffuses with simple production/decay terms
- Following cell-kinetic models (e.g. HILLEN, PAINTER (2009) *J. Math. Biol.* 58) we assume small cell/zoospore diffusivity regime
- The model is not predictive; intends to understand the underlying dynamics

System of equations:

$$
\begin{aligned}
u_t &= D_u \Delta u + \lambda u(u_0 - u)(u - u_*) - \nabla \cdot J_c, \\
v_t &= D_v \Delta v + \beta v(v_0 - v)(v - v_*), \\
c_t &= D_c \Delta c + \delta v - \alpha c,
\end{aligned}
$$

where u - concentration density of pathogen; v - of bacteria; and, c - of the chemo-repellent.

$x \in \Omega \subset \mathbb{R}^2$, $t \geq 0$, $D_{u,c,v} > 0$ diffusion coefficients; $\alpha, \beta, \delta, \lambda > 0$.

$0 < u_* < u_0$, $0 < v_* < v_0$.

$$
\begin{aligned}
&\Omega = [0, L] \times [0, L] \\
\text{or,} \quad &\Omega = \{x^2 + y^2 \leq L^2/\pi\}, \quad L > 0.
\end{aligned}
$$

System of equations:

$$
\begin{aligned}
u_t &= D_u \Delta u + \lambda u(u_0 - u)(u - u_*) - \nabla \cdot J_c, \\
v_t &= D_v \Delta v + \beta v(v_0 - v)(v - v_*), \\
c_t &= D_c \Delta c + \delta v - \alpha c,
\end{aligned}
$$

where u - concentration density of pathogen; v - of bacteria; and, c - of the chemo-repellent.

$x \in \Omega \subset \mathbb{R}^2$, $t \geq 0$, $D_{u,c,v} > 0$ diffusion coefficients; $\alpha, \beta, \delta, \lambda > 0$.

$0 < u_* < u_0$, $0 < v_* < v_0$.

$$
\begin{aligned}
&\Omega = [0, L] \times [0, L] \\
\text{or,} \quad &\Omega = \{x^2 + y^2 \leq L^2/\pi\}, \quad L > 0.
\end{aligned}
$$

System of equations:

$$
\begin{aligned}
u_t &= D_u \Delta u + \lambda u(u_0 - u)(u - u_*) - \nabla \cdot J_c, \\
v_t &= D_v \Delta v + \beta v(v_0 - v)(v - v_*), \\
c_t &= D_c \Delta c + \delta v - \alpha c,
\end{aligned}
$$

where u - concentration density of pathogen; v - of bacteria; and, c - of the chemo-repellent.

$x \in \Omega \subset \mathbb{R}^2$, $t \geq 0$, $D_{u,c,v} > 0$ diffusion coefficients; $\alpha, \beta, \delta, \lambda > 0$.

$0 < u_* < u_0$, $0 < v_* < v_0$.

$$
\begin{aligned}
&\Omega = [0, L] \times [0, L] \\
\text{or,} \quad &\Omega = \{x^2 + y^2 \leq L^2/\pi\}, \quad L > 0.
\end{aligned}
$$

No-flux boundary conditions:

$$\nabla u \cdot \hat{n} = 0, \quad \nabla v \cdot \hat{n} = 0, \quad \nabla c \cdot \hat{n} = 0, \quad \text{at } \partial\Omega.$$

Chemotaxis:

$$J_c = -u\chi(c)\nabla c,$$

$\chi(c)$ - chemotactic sensitivity. Simplest choice: uniform response to chemosensory stimulus (KELLER, SEGEL (1971)):

$$\chi(c) \equiv \chi_0 > 0, \quad \text{constant.} \qquad J_c = -\chi_0 uc\nabla c.$$

Negative sign: chemo-repellent (negative chemotaxis).

No-flux boundary conditions:

$$\nabla u \cdot \hat{n} = 0, \quad \nabla v \cdot \hat{n} = 0, \quad \nabla c \cdot \hat{n} = 0, \quad \text{at } \partial\Omega.$$

Chemotaxis:

$$J_c = -u\chi(c)\nabla c,$$

$\chi(c)$ - chemotactic sensitivity. Simplest choice: uniform response to chemosensory stimulus (KELLER, SEGEL (1971)):

$$\chi(c) \equiv \chi_0 > 0, \quad \text{constant.} \qquad J_c = -\chi_0 uc\nabla c.$$

Negative sign: chemo-repellent (negative chemotaxis).

Non-dimensionalization:

$$D_u \to \frac{D_u}{2D_c},\ D_v \to \frac{D_v}{2D_c},\ t \to \alpha t,\ x \to \sqrt{\frac{\alpha}{2D_c}}x,\ y \to \sqrt{\frac{\alpha}{2D_c}}y,$$

$$c \to \frac{c}{c_0}, \quad u \to \frac{u}{u_0}, \quad v \to \frac{v}{v_0}, \quad u_* \to \frac{u_*}{u_0}, \quad v_* \to \frac{v_*}{v_0},$$

$$\lambda \to \lambda\frac{u_0^2}{\alpha}, \quad \beta \to \beta\frac{v_0^2}{\alpha}, \quad \delta \to \delta\frac{v_0}{c_0\alpha}, \quad \gamma \to \chi_0\frac{c_0}{2D_c}.$$

Non-dimensional system:

$$
\begin{aligned}
u_t &= D_u \Delta u + \lambda u(1-u)(u-u_*) + \gamma \nabla \cdot (u \nabla c), \\
v_t &= D_v \Delta v + \beta v(1-v)(v-v_*), \\
c_t &= \tfrac{1}{2}\Delta c + \delta v - c.
\end{aligned}
$$

W.l.o.g. $L\sqrt{2D_c/\alpha} = O(1)$. Domain:

$$\Omega = [0,1] \times [0,1], \qquad \text{or,} \qquad \Omega = \{x^2 + y^2 \leq 1/\pi\}.$$

Features:

- Triangular (essentially scalar) system of RDC equations.
- Simplest chemotactic interaction (repulsion).
- Small diffusion ($D_{u,v} \ll 1$) regime; $D_c = O(1)$.
- Logistics growth with a threshold.

1 An experiment

2 Modeling

3 Asymptotic analysis

4 Numerical simulations

Front asymptotics

Small diffusion regime $D_u \approx 0$: layers are well-approximated by interfaces (small width).

Front:

$$\Sigma(t) = \{(x,y) \in \Omega : u(x,y,t) = u_2\},$$

$$\Omega_{\text{in}} = \{(x,y) \in \Omega : u(x,y,t) < u_2\},$$
$$\Omega_{\text{out}} = \{(x,y) \in \Omega : u(x,y,t) > u_2\}.$$

Local curvilinear coordinates: $\zeta(x,y,t)$ (normal); $\tau(x,y,t)$ (tangential). $|\nabla\zeta| = |\nabla\tau| = 1$.

Approximation: $u(x,y,t) \approx \bar{u}(\zeta(x,y,t))$.

ODE for $\bar{u}$:

$$(-s+D_u\kappa-\gamma\nabla\zeta\cdot\nabla c_\Sigma)\bar{u}' = D_u\bar{u}'' + \lambda\bar{u}(\bar{u}-u_*)(1-\bar{u}) + \gamma\Delta c_\Sigma\bar{u},$$

$s = -\partial_t\zeta$ (normal velocity); $\kappa = -\Delta\zeta$ (local curvature).

For stable or metastable states: v, c and Δc at Σ are approx. time-independent.

ODE for $\bar{u}$:

$$(-s+D_u\kappa-\gamma\nabla\zeta\cdot\nabla c_\Sigma)\bar{u}' = D_u\bar{u}'' + \lambda\bar{u}(\bar{u}-u_*)(1-\bar{u}) + \gamma\Delta c_\Sigma\bar{u},$$

$s = -\partial_t\zeta$ (normal velocity); $\kappa = -\Delta\zeta$ (local curvature).

For stable or metastable states: v, c and Δc at Σ are approx. time-independent.

Interface equation of motion

ODE has the form of a Nagumo front:

$$-s_1\bar{u}' = D_u\bar{u}'' + \lambda\bar{u}(u_1-\bar{u})(\bar{u}-u_2),$$

$$u_1 = \tfrac{1}{2}(1+u_*) + \tfrac{1}{2}\sqrt{(1-u_*)^2 + 4\gamma\Delta c_\Sigma/\lambda} \approx 1 + \frac{\gamma}{\lambda(1-u_*)}\Delta c_\Sigma,$$
$$u_2 = \tfrac{1}{2}(1+u_*) - \tfrac{1}{2}\sqrt{(1-u_*)^2 + 4\gamma\Delta c_\Sigma/\lambda} \approx u_* - \frac{\gamma}{\lambda(1-u_*)}\Delta c_\Sigma.$$

Computation of the Nagumo speed s_1: $\bar{u}' = \phi(\bar{u})$, $\phi(0) = \phi(u_1) = 0$, $\phi < 0$. Solution: $\phi(\bar{u}) = -\mu\bar{u}(u_1-\bar{u})$, with $\mu = \sqrt{\lambda/2D_u} > 0$.

$$s_1 = \sqrt{2\lambda D_u}\left(\tfrac{1}{2}u_1 - u_2\right).$$

Interface equation of motion

ODE has the form of a Nagumo front:

$$-s_1\bar{u}' = D_u\bar{u}'' + \lambda\bar{u}(u_1-\bar{u})(\bar{u}-u_2),$$

$$\begin{aligned} u_1 &= \tfrac{1}{2}(1+u_*) + \tfrac{1}{2}\sqrt{(1-u_*)^2 + 4\gamma\Delta c_\Sigma/\lambda} \approx 1 + \tfrac{\gamma}{\lambda(1-u_*)}\Delta c_\Sigma, \\ u_2 &= \tfrac{1}{2}(1+u_*) - \tfrac{1}{2}\sqrt{(1-u_*)^2 + 4\gamma\Delta c_\Sigma/\lambda} \approx u_* - \tfrac{\gamma}{\lambda(1-u_*)}\Delta c_\Sigma. \end{aligned}$$

Computation of the Nagumo speed s_1: $\bar{u}' = \phi(\bar{u})$, $\phi(0) = \phi(u_1) = 0$, $\phi < 0$. Solution: $\phi(\bar{u}) = -\mu\bar{u}(u_1-\bar{u})$, with $\mu = \sqrt{\lambda/2D_u} > 0$.

$$s_1 = \sqrt{2\lambda D_u}\left(\tfrac{1}{2}u_1 - u_2\right).$$

Chemotactic velocity:

$$s_2 = \gamma \nabla \zeta \cdot \nabla c = \gamma \frac{dc}{d\zeta}.$$

Interface equation of motion:

$$s = s_1 - \gamma \frac{dc}{d\zeta} + D_u \kappa.$$

The sign of s_1 is that of

$$u_1 - 2u_2 \approx 1 - 2u_* + 3\gamma \Delta c_\Sigma / \lambda (1 - u_*).$$

Chemotactic velocity:

$$s_2 = \gamma \nabla \zeta \cdot \nabla c = \gamma \frac{dc}{d\zeta}.$$

Interface equation of motion:

$$s = s_1 - \gamma \frac{dc}{d\zeta} + D_u \kappa.$$

The sign of s_1 is that of

$$u_1 - 2u_2 \approx 1 - 2u_* + 3\gamma \Delta c_\Sigma / \lambda (1 - u_*).$$

Example: circular front.

$\Sigma(t) = \{\sqrt{x^2+y^2} = R(t)\}$. $\zeta = R(t) - r$, $\kappa = -\Delta\zeta = 1/r$.

Normal speed $s = -\partial_t \zeta = -\dot{R}(t)$; $dc/d\zeta = -dc/dr$.

Yields:

$$\dot{R}(t) = -\sqrt{2\lambda D_u}\left(\tfrac{1}{2}u_1 - u_2\right) - \left(\gamma\frac{dc}{dr} + \frac{D_u}{r}\right)_{|r=R(t)}$$

Necessary condition for equilibrium:

$$\dot{R}(t) = 0, \qquad \text{at } \Sigma.$$

Example: circular front.

$\Sigma(t) = \{\sqrt{x^2+y^2} = R(t)\}$. $\zeta = R(t) - r$, $\kappa = -\Delta\zeta = 1/r$.

Normal speed $s = -\partial_t \zeta = -\dot{R}(t)$; $dc/d\zeta = -dc/dr$.

Yields:

$$\dot{R}(t) = -\sqrt{2\lambda D_u}\left(\tfrac{1}{2}u_1 - u_2\right) - \left(\gamma\frac{dc}{dr} + \frac{D_u}{r}\right)_{|r=R(t)}$$

Necessary condition for equilibrium:

$$\dot{R}(t) = 0, \qquad \text{at } \Sigma.$$

Stationary solutions

For simplicity

$$\Omega = \{x^2 + y^2 \leq 1/\pi\}.$$

Stationary equation:

$$0 = D_v \Delta v + \beta v(1-v)(v - v_*), \qquad \text{in } \Omega.$$

+ no-flux b.c. Initial condition for v:

$$v(x,y,0) = Ae^{-\omega r^2},$$

$$1 < \frac{A}{v_*} < e^{\omega/\pi}.$$

Radially symmetric stationary/meta-stable solution $v = v_\infty(r)$.

Stationary solutions

For simplicity

$$\Omega = \{x^2 + y^2 \leq 1/\pi\}.$$

Stationary equation:

$$0 = D_v \Delta v + \beta v(1-v)(v - v_*), \qquad \text{in } \Omega.$$

+ no-flux b.c. Initial condition for v:

$$v(x,y,0) = Ae^{-\omega r^2},$$

$$1 < \frac{A}{v_*} < e^{\omega/\pi}.$$

Radially symmetric stationary/meta-stable solution $v = v_\infty(r)$.

Stationary solutions for c:

$$\begin{aligned} &\tfrac{1}{2}\Delta c + \delta v_\infty - c = 0, && \text{in } \Omega, \\ &\nabla c \cdot \hat{n} = 0, && \text{at } \partial\Omega. \end{aligned}$$

Cases:

- $D_v = 0$ (zero-diffusion)
- $0 < D_v \ll 1$ (small-diffusion regime)

Stationary solutions for c:

$$\begin{aligned} &\tfrac{1}{2}\Delta c + \delta v_\infty - c = 0, && \text{in } \Omega, \\ &\nabla c \cdot \hat{n} = 0, && \text{at } \partial\Omega. \end{aligned}$$

Cases:

- $D_v = 0$ (zero-diffusion)
- $0 < D_v \ll 1$ (small-diffusion regime)

Case 1: Zero-diffusion

The v-equation is an ODE. Stationary solution is the *plateau*:

$$v_\infty(r) = \begin{cases} 1, & 0 < r < R_1, \\ 0, & R_1 < r < 1/\sqrt{\pi}, \end{cases},$$

$$R_1 = \sqrt{\omega^{-1} \log(A/v_*)}.$$

Solution for c:

$$c(r) = \begin{cases} C_1 I_0(\sqrt{2}r) + C_2 K_0(\sqrt{2}r), & R_1 < r < 1/\sqrt{\pi}, \\ C_3 I_0(\sqrt{2}r) + \delta, & 0 < r < R_1, \end{cases}$$

$$C_1 = \sqrt{2}\delta R_1 \frac{K_1(\sqrt{2/\pi}) I_1(\sqrt{2}R_1)}{I_1(\sqrt{2/\pi})},$$

$$C_2 = \sqrt{2}\delta R_1 I_1(\sqrt{2}R_1),$$

$$C_3 = \frac{\sqrt{2}\delta R_1}{I_1(\sqrt{2/\pi})} \Big(K_1(\sqrt{2/\pi}) I_1(\sqrt{2}R_1) - I_1(\sqrt{2/\pi}) K_1(\sqrt{2}R_1) \Big)$$

K_n, I_n modified Bessel functions.

Case 2: small-diffusion

When $0 < D_v$, solutions with Neumann b.c. converge to stable equilibrium solutions (CASTEN, HOLLAND, *SIAM J. Appl. Math* (1977), *J. Diff. Eqs.* (1978))

If $D_v \ll 1$ the convergence is *very slow*. Solutions may exhibit meta-stability (Ref. CARR, PEGO, *Comm. Pure Appl. Math* (1989); *Proc. Roy. Soc. Edinburgh A* (1990). Bi-stable RD equation in 1-d.)

Transient patterns for bi-stable RD equation in 2-d: Slowly evolving, not local minimizers nor necessarily close to equilibria, apparently stable, transient time increases depending on size of domian, D_v and β.

Case 2: small-diffusion

When $0 < D_v$, solutions with Neumann b.c. converge to stable equilibrium solutions (CASTEN, HOLLAND, *SIAM J. Appl. Math* (1977), *J. Diff. Eqs.* (1978))

If $D_v \ll 1$ the convergence is *very slow*. Solutions may exhibit meta-stability (Ref. CARR, PEGO, *Comm. Pure Appl. Math* (1989); *Proc. Roy. Soc. Edinburgh A* (1990). Bi-stable RD equation in 1-d.)

Transient patterns for bi-stable RD equation in 2-d: Slowly evolving, not local minimizers nor necessarily close to equilibria, apparently stable, transient time increases depending on size of domian, D_v and β.

Case 2: small-diffusion

When $0 < D_v$, solutions with Neumann b.c. converge to stable equilibrium solutions (CASTEN, HOLLAND, *SIAM J. Appl. Math* (1977), *J. Diff. Eqs.* (1978))

If $D_v \ll 1$ the convergence is *very slow*. Solutions may exhibit meta-stability (Ref. CARR, PEGO, *Comm. Pure Appl. Math* (1989); *Proc. Roy. Soc. Edinburgh A* (1990). Bi-stable RD equation in 1-d.)

Transient patterns for bi-stable RD equation in 2-d: Slowly evolving, not local minimizers nor necessarily close to equilibria, apparently stable, transient time increases depending on size of domian, D_v and β.

Assumptions:

- The meta-stable patterns for v when $D_v \ll 1$ is small induce meta-stable patterns in u and c.
- These transient solutions are well-approximated by the stationary solutions computed when $D_v = 0$.

Let $r = R_0 < 1/\pi$ interface equilibrium position. Suppose that either:

- $R(t) \to R_0$ as $t \to +\infty$ in the zero-diffusion case $D_v = 0$, or,
- There exist $0 < T_0 = O(1/\lambda) \ll T_1 = T_1(D_v, L, \beta)$, uniform $\varepsilon > 0$ such that

$$|R(t) - R_0| \leq \varepsilon, \qquad t \in [T_0, T_1]$$

Assumptions:

- The meta-stable patterns for v when $D_v \ll 1$ is small induce meta-stable patterns in u and c.
- These transient solutions are well-approximated by the stationary solutions computed when $D_v = 0$.

Let $r = R_0 < 1/\pi$ interface equilibrium position. Suppose that either:

- $R(t) \to R_0$ as $t \to +\infty$ in the zero-diffusion case $D_v = 0$, or,
- There exist $0 < T_0 = O(1/\lambda) \ll T_1 = T_1(D_v, L, \beta)$, uniform $\varepsilon > 0$ such that

$$|R(t) - R_0| \leq \varepsilon, \qquad t \in [T_0, T_1]$$

In both zero- and small-diffusion limits, condition for equilibrium:

$$\dot{R}(t)_{|r=R_0} = -\sqrt{2\lambda D_u}\left(\tfrac{1}{2}u_1 - u_2\right) - \frac{D_u}{R_0} - \gamma c'(R_0) = 0$$

Take ω large s.t. $R_1 < R_0$. Thus, $v_\infty(R_0) = 0$ and we may approximate:

$$\Delta c_{\Sigma|r=R_0} \approx 2c(R_0)$$

$$u_1 \approx 1 + \frac{2\gamma}{\lambda(1-u_*)}c(R_0)$$

$$u_2 \approx u_* - \frac{2\gamma}{\lambda(1-u_*)}c(R_0)$$

In both zero- and small-diffusion limits, condition for equilibrium:

$$\dot{R}(t)_{|r=R_0} = -\sqrt{2\lambda D_u}\left(\tfrac{1}{2}u_1 - u_2\right) - \frac{D_u}{R_0} - \gamma c'(R_0) = 0$$

Take ω large s.t. $R_1 < R_0$. Thus, $v_\infty(R_0) = 0$ and we may approximate:

$$\Delta c_{\Sigma|r=R_0} \approx 2c(R_0)$$

$$u_1 \approx 1 + \frac{2\gamma}{\lambda(1-u_*)}c(R_0)$$

$$u_2 \approx u_* - \frac{2\gamma}{\lambda(1-u_*)}c(R_0)$$

From asymptotics of K_0, I_0, K_1, I_1:

$$
\begin{aligned}
c(R_0) &\approx C_1\left(1+\tfrac{1}{2}R_0^2\right) + C_2(\log\sqrt{2} - \tilde{\varepsilon} - \log R_0),\\
c'(R_0) &\approx C_1 R_0 - C_2/R_0\\
u_2 - \tfrac{1}{2}u_1 &\approx u_* - \frac{1}{2} - \frac{3\gamma}{\lambda(1-u_*)}\Big[C_1\left(1+\tfrac{1}{2}R_0^2\right)\\
&\qquad + C_2(\log\sqrt{2} - \tilde{\varepsilon} - \log R_0)\Big]
\end{aligned}
$$

$\tilde{\varepsilon} =$ Euler const. ≈ 0.5772.

Upon substitution:

$$p(R_0) = 0$$

where

$$p(x) := a_3x^3 + a_2x^2 + a_1x + a_0 + bx\log x$$

$$a_3 = \sqrt{\lambda D_u}\frac{3\gamma C_1}{\sqrt{2}\lambda(1-u_*)} = \frac{3\gamma C_1\sqrt{D_u}}{\sqrt{2\lambda}(1-u_*)},$$

$$a_2 = \gamma C_1,$$

$$a_1 = \sqrt{2\lambda D_u}\Big(\frac{1}{2} - u_* + \frac{3\gamma}{\lambda(1-u_*)}\big(C_1 + C_2(\log\sqrt{2} - \tilde{\varepsilon})\big)\Big),$$

$$a_0 = D_u - \gamma C_2,$$

$$b = -\sqrt{2\lambda D_u}\frac{3\gamma C_2}{\lambda(1-u_*)} = -\frac{3\gamma C_2\sqrt{2D_u}}{\sqrt{\lambda}(1-u_*)}.$$

It can be solved numerically.

Example: If $A = 3$, $\omega = 1000$, $\delta = 10$, $D_u = 0.01$, $v_* = 0.5$ then

$$R_1 = 0.0423$$
$$R_0 \approx 0.1315$$
$$\gamma c''(R_0) \approx 3.4409$$
$$\frac{D_u}{R_0^2} \approx 0.5783$$

Linearized stability

Formal computations: is the equilibrium front stable?

Radial perturbations: $R_0 + \eta(t)$, $\eta \ll 1$ (perturbation).
Linerized eqn.:

$$\dot{\eta}(t) = \left(\frac{D_u}{R_0^2} - \gamma c''(R_0)\right)\eta$$

Linearly stable under radial perturbations if
$\gamma c''(R_0) > D_u/R_0^2$.

Linearized stability

Formal computations: is the equilibrium front stable?

Radial perturbations: $R_0 + \eta(t)$, $\eta \ll 1$ (perturbation).
Linerized eqn.:

$$\dot{\eta}(t) = \left(\frac{D_u}{R_0^2} - \gamma c''(R_0)\right)\eta$$

Linearly stable under radial perturbations if
$\gamma c''(R_0) > D_u/R_0^2$.

Azimuthally dependent perturbations:

Interface $X(\theta,t) = (x,y)(\theta,t)$. Eqn. of motion:

$$X_t = \big(c - D_u \kappa(\theta,t) - \nabla c(X(\theta,t)) \cdot \hat{n}\big)\hat{n},$$

$$\kappa(\theta,t) = \frac{x_\theta y_{\theta\theta} - y_\theta x_{\theta\theta}}{(x_\theta^2 + y_\theta^2)^{3/2}}$$

(local curvature).

Steady states:

$$c - D_u \kappa(\theta) - \nabla c(X(\theta)) \cdot \hat{n} = 0$$

Provides an eqn. for X.

Azimuthally dependent perturbations:

Interface $X(\theta,t) = (x,y)(\theta,t)$. Eqn. of motion:

$$X_t = \big(c - D_u \kappa(\theta,t) - \nabla c(X(\theta,t)) \cdot \hat{n}\big)\hat{n},$$

$$\kappa(\theta,t) = \frac{x_\theta y_{\theta\theta} - y_\theta x_{\theta\theta}}{(x_\theta^2 + y_\theta^2)^{3/2}}$$

(local curvature).

Steady states:

$$c - D_u \kappa(\theta) - \nabla c(X(\theta)) \cdot \hat{n} = 0$$

Provides an eqn. for X.

Linearized stability: $X(\theta,t) = X_0(\theta) + \xi(\theta,t)$. Upon subst.

$$\xi_t = \frac{1}{|X_0'|^3}\left(3\kappa_0 \frac{X_0' \cdot \xi'}{|X_0'|^2} - (X_0')^\perp \cdot \xi'' - X_0'' \cdot (\xi')^\perp\right)\hat{n}_0 - \gamma(\xi', (D^2 c)\hat{n}_0),$$

$' = d/d\theta$. $D^2 c$ - Hessian. Local coordinates:

$$\xi = p(\theta,t)\hat{\tau}_0(\theta) + q(\theta,t)\hat{n}_0(\theta).$$

Thus $p_t = 0$ (or, $p = 0$: change in parametrization). Eqn. for q with periodic b.c.

$$q_t = \frac{D_u}{R_0^2} q_{\theta\theta} + \left(\frac{D_u}{R_0^2} - \gamma c''(R_0)\right) q.$$

Decay of azimuthal perturbations if $\gamma c''(R_0) > D_u/R_0^2$.

Linearized stability: $X(\theta,t) = X_0(\theta) + \xi(\theta,t)$. Upon subst.

$$\xi_t = \frac{1}{|X_0'|^3}\left(3\kappa_0 \frac{X_0' \cdot \xi'}{|X_0'|^2} - (X_0')^\perp \cdot \xi'' - X_0'' \cdot (\xi')^\perp\right)\hat{n}_0 - \gamma(\xi', (D^2 c)\hat{n}_0),$$

$' = d/d\theta$. $D^2 c$ - Hessian. Local coordinates:

$$\xi = p(\theta,t)\hat{\tau}_0(\theta) + q(\theta,t)\hat{n}_0(\theta).$$

Thus $p_t = 0$ (or, $p = 0$: change in parametrization). Eqn. for q with periodic b.c.

$$q_t = \frac{D_u}{R_0^2} q_{\theta\theta} + \left(\frac{D_u}{R_0^2} - \gamma c''(R_0)\right) q.$$

Decay of azimuthal perturbations if $\gamma c''(R_0) > D_u/R_0^2$.

1 An experiment

2 Modeling

3 Asymptotic analysis

4 Numerical simulations

Numerical simulations

Parameter values used in simulations:

Description	Symbol	Value
Diffusion coefficient of u	D_u	0.01
Diffusion coefficient of v	D_v	10^{-5} or 0
Rate of production of c	δ	10.0
Reaction coefficient of v	β	8.0
Reaction coefficient of u	λ	60.0
Chemotactic sensitivity	γ	3.2
Unstable equilibrium for u	u_*	0.2
Unstable equilibrium for v	v_*	0.5

Euler explicit scheme.

Domain:

$$0 \leq x \leq 1, \quad 0 \leq y \leq 1$$

$$\Delta x = \Delta y = \frac{1}{N-1} \approx 3.9 \times 10^{-3}, \qquad N = 256.$$

Time step:

$$\Delta t = 10^{-3} \times \Delta x \approx 3.9 \times 10^{-6}.$$

Courant no. $\mu \Delta t / (\Delta x)^2 \approx 0.25$ (numerical stability).

x, y, t in arbitrary units (AU).

Very small time steps to avoid instabilities (stiffness). Compensated by the use of Graphic Processing Units (GPUs). Parallel high performance computations with 100s of processors. NVIDIA© GeForce GTx 480 (millions of time steps in a few hours).

Simulation no. 1: zero-diffusion $D_v = 0$

$A = 3$, $\omega = 1000$ and $v_* = 0.5$. Initial conditions:

$$v(x,y,0) = 3e^{-1000((x-0.5)^2+(y-0.5)^2)}$$

$$c(x,y,0) = 0$$

$$u(x,y,0) = 10\left(e^{1000((x-0.2)^2+(y-0.2)^2)} + e^{-1000((x-0.2)^2+(y-0.2)^2)}\right)^{-1}$$

Formation if sharp plateau for v concentration. Numerical radius: $R_1 \approx 0.0412$ (error 2.6%).

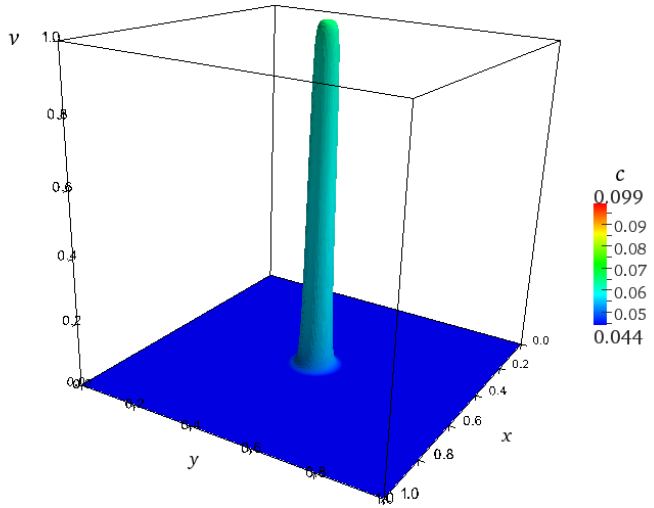

(a) $t = 0.1961$.

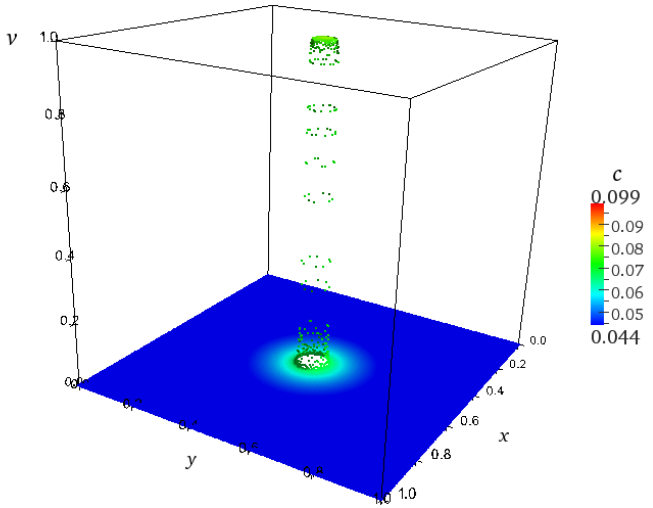

(b) $t = 0.9804$.

Stationary solution for $t \geq 9$ (plateau).

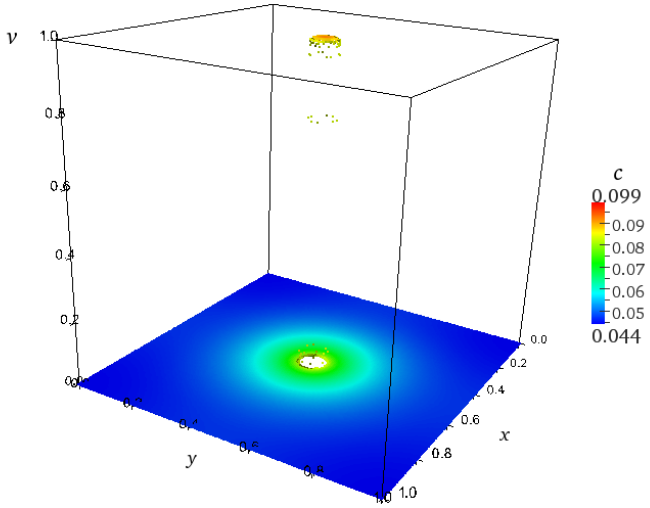

(c) $t = 1.9608$.

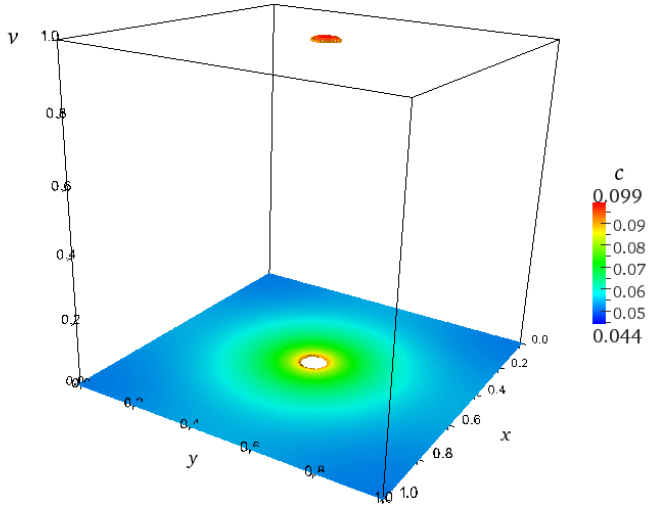

(d) $t = 9.8039$.

Figure: Figures (a) - (d) show concentration v in the zero-diffusion limit $D_v = 0$. Stationary state depicted in (d).

Induced stationary state for c concentration at time $t = 9.8039$.

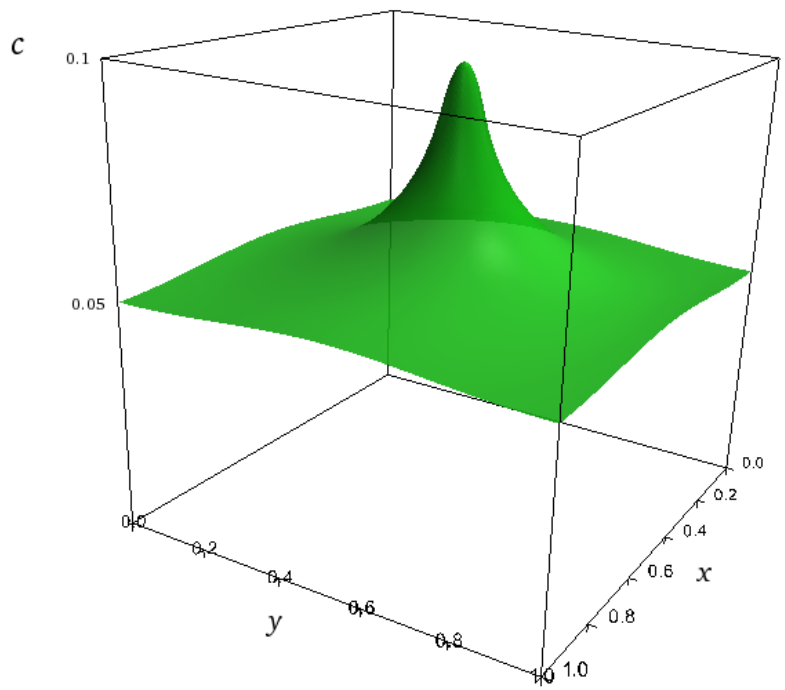

Concentration u ($D_v = 0$ case) for different times. Arbitrary initial condition at time $t = 0$ (see (a), for $t = 0.1962$).

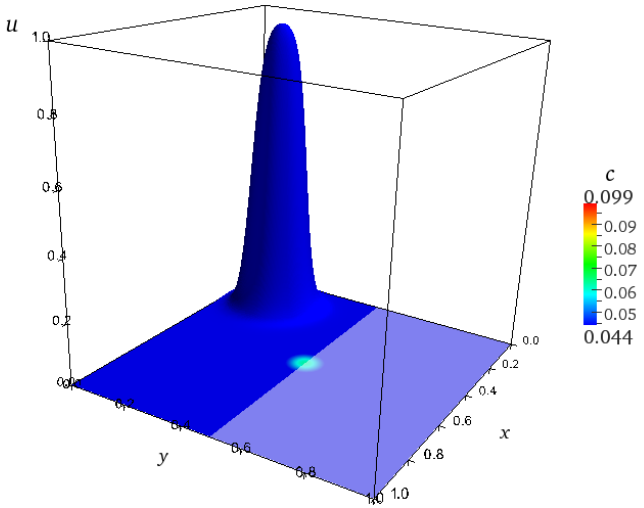

(a) $t = 0.1961$.

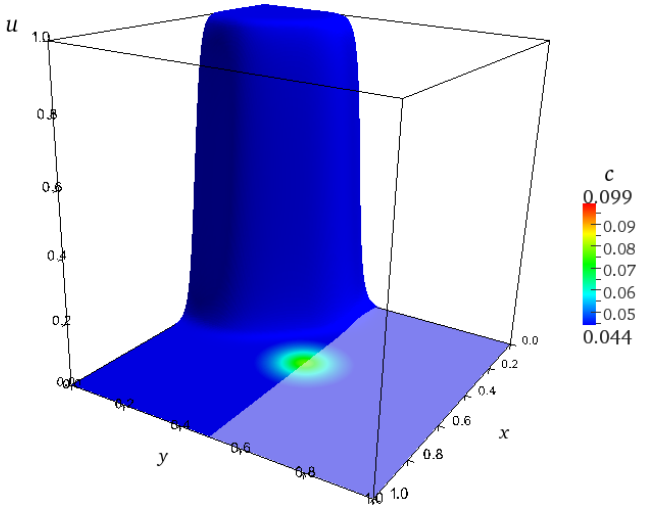

(b) $t = 0.7843$.

Invasive front in u variable; it senses the chemo-repellent concentrated in the center of the domain.

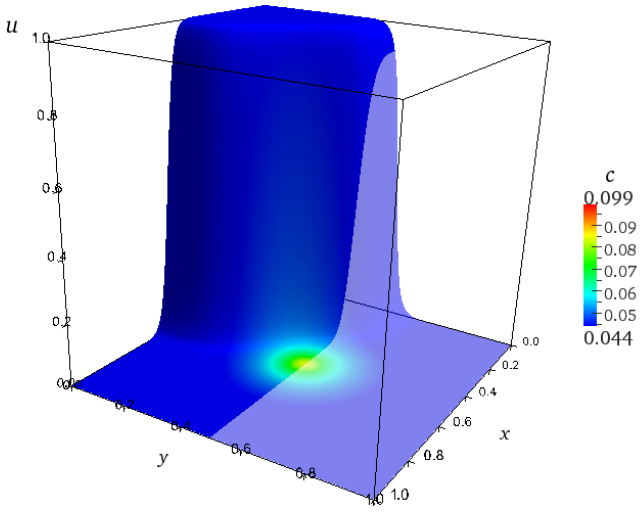

(c) $t = 1.1765.$

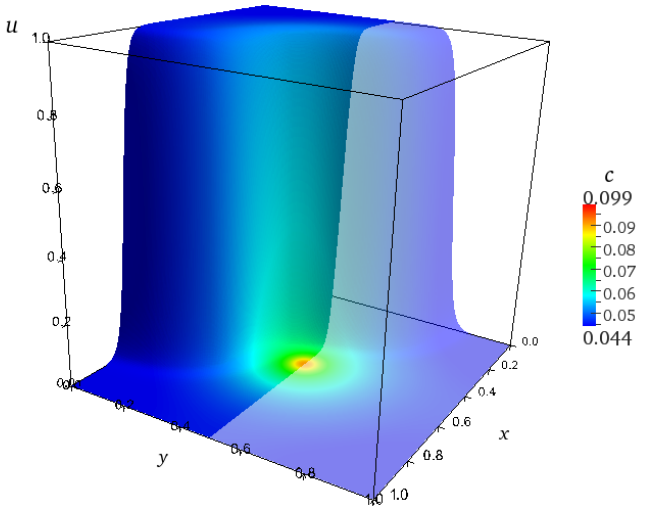

(d) $t = 1.7647.$

Invasive circular front.

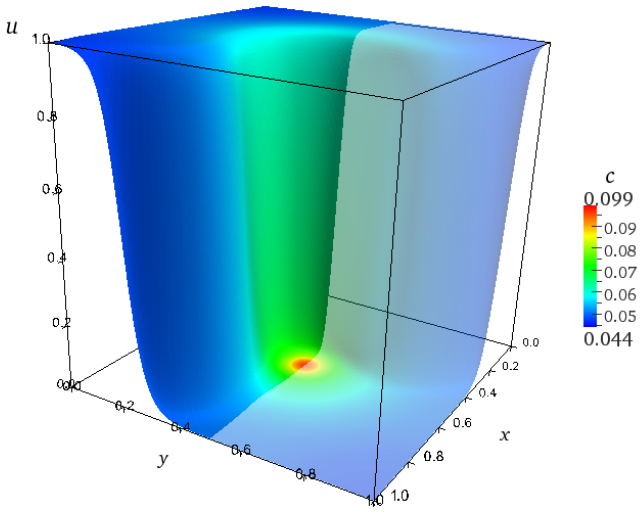

(e) $t = 3.9216.$

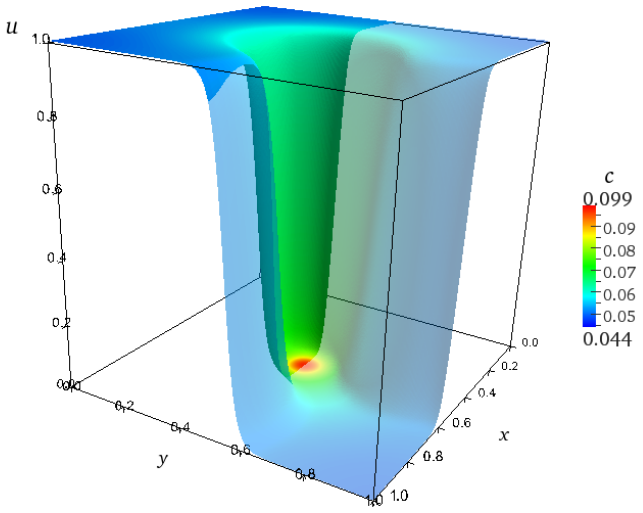

(f) $t = 9.8039.$

The concentration u reaches a stationary state (equilibrium circular front) when $t > 9$.

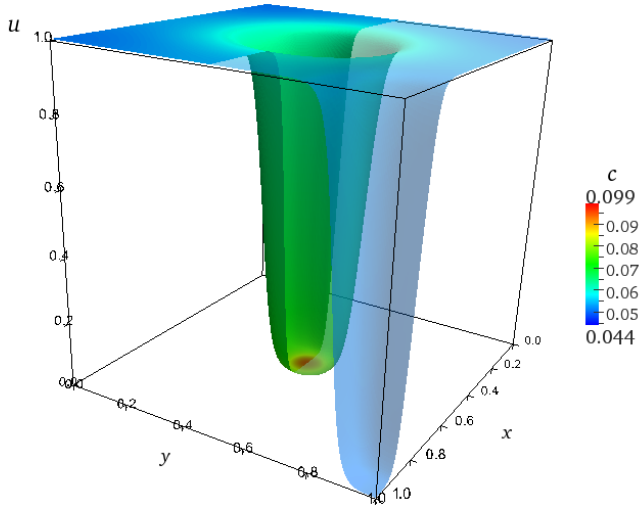

(g) $t = 3.9216$.

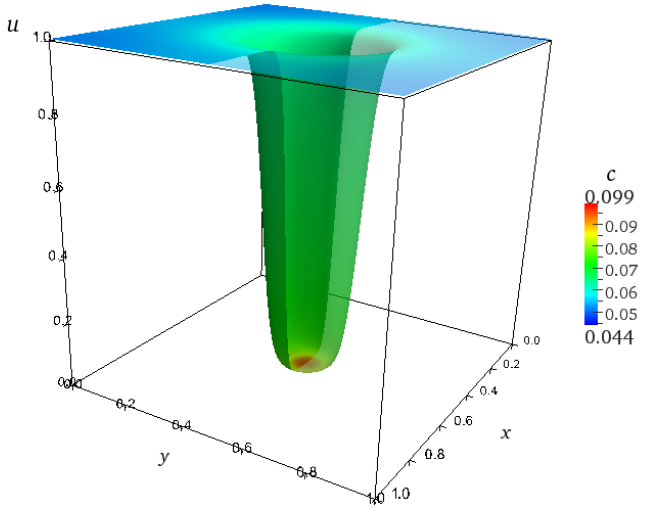

(h) $t = 9.8039$.

Figure: Invasive front for u concentration in the zero-diffusion limit for v ($D_v = 0$). Reaches stationary state in (h).

Top view of stationary front in u (time $t = 9.8039$). Numerically estimated equilibrium radius $R_0 = 0.1235$ (relative error 6%).

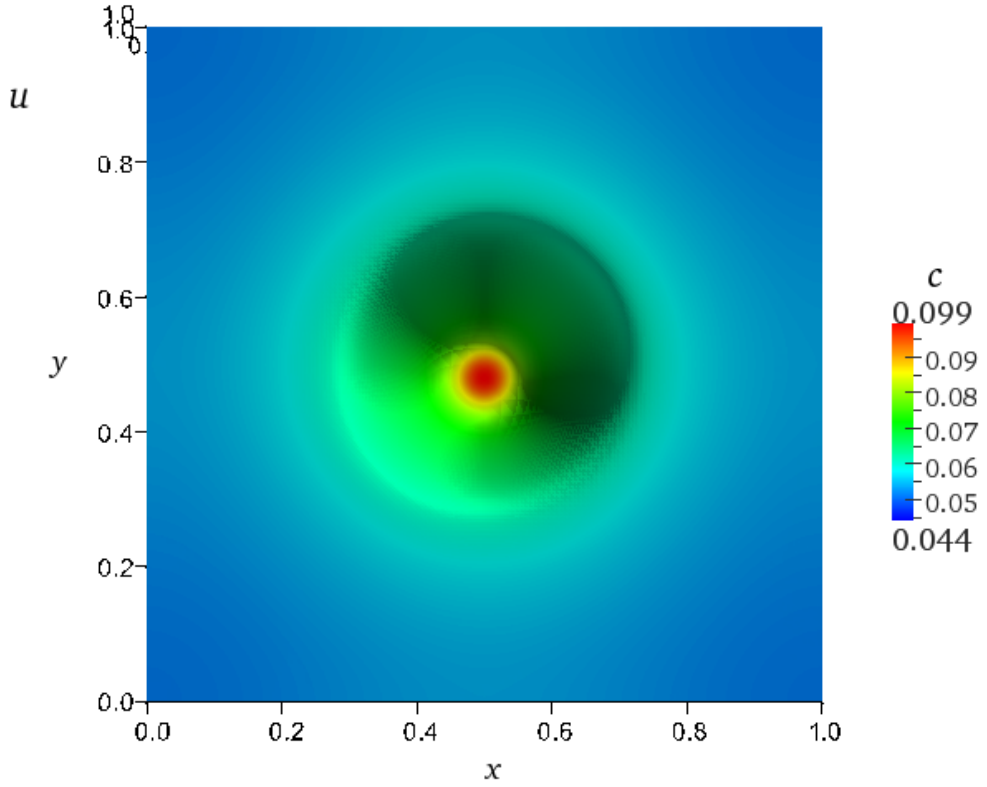

Simulation no. 2: small-diffusion $0 < D_v \ll 1$

Same initial conditions as in simulation no. 1. Here:

$$D_v = 10^{-5}$$

Solutions tend to equilibria $v = 0$ or $v = 1$ as $t \to +\infty$.
Results: Larger time scale; existence of a transient layer that resembles the stationary solutions in the zero-diffusion regime.

Simulation no. 2: small-diffusion $0 < D_v \ll 1$

Same initial conditions as in simulation no. 1. Here:

$$D_v = 10^{-5}$$

Solutions tend to equilibria $v = 0$ or $v = 1$ as $t \to +\infty$.
Results: Larger time scale; existence of a transient layer that resembles the stationary solutions in the zero-diffusion regime.

Concentration v for small-diffusion. In (b): smooth transient layer that persists until $t \sim 100$.

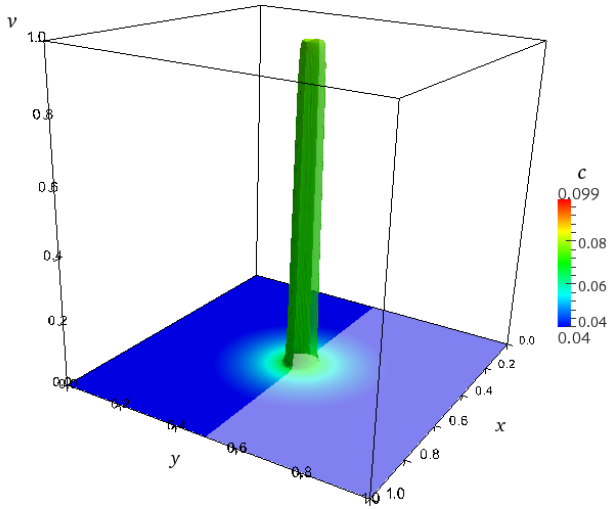

(a) $t = 0.980$.

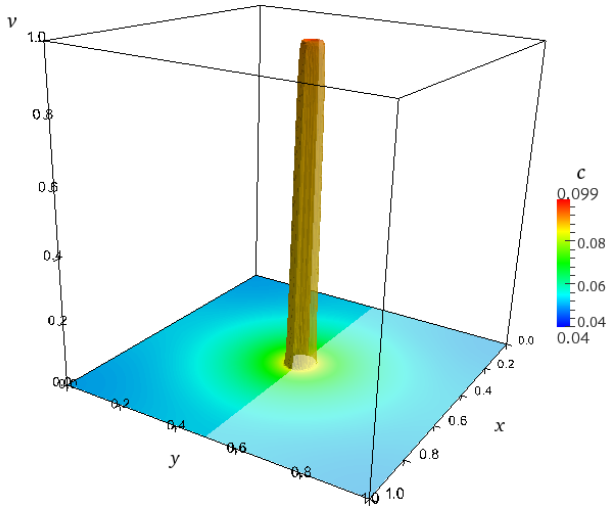

(b) $t = 9.804$.

Concentration v for large times. Solution eventually tends to equilibrium $v = 0$, for $t > 180$.

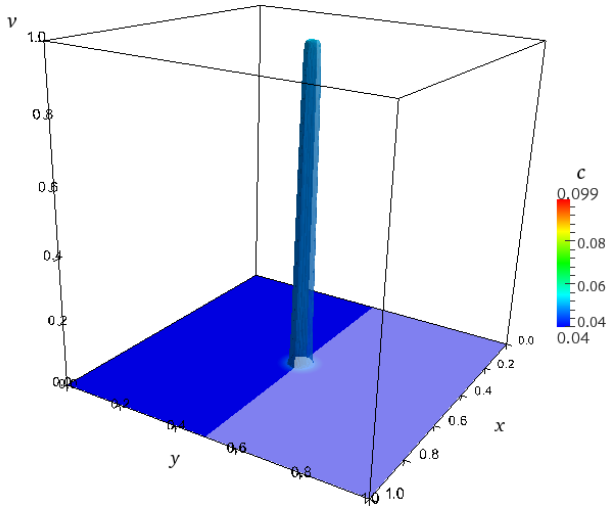

(c) $t = 99.020$.

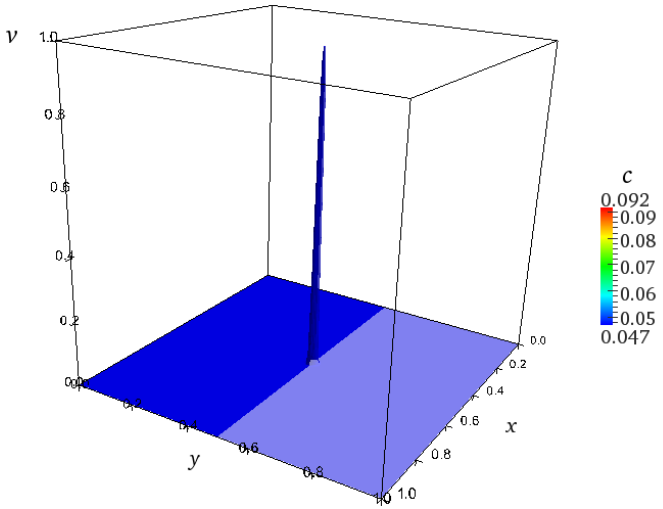

(d) $t = 166.667$.

Figure: Concentration v in the small-diffusion regime with $D_v = 10^{-5}$. Solution eventually tends to $v = 0$.

Concentration c (small-diffusion for v). Transient pattern reached before time $t = 0.980$. Figure (a) depicts transient layer at time $t = 9.8039$ (figure (a)); it persists for long times.

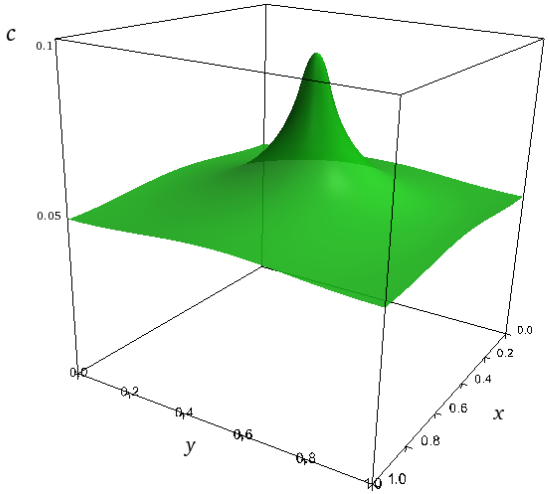

(a) $t = 9.8039$.

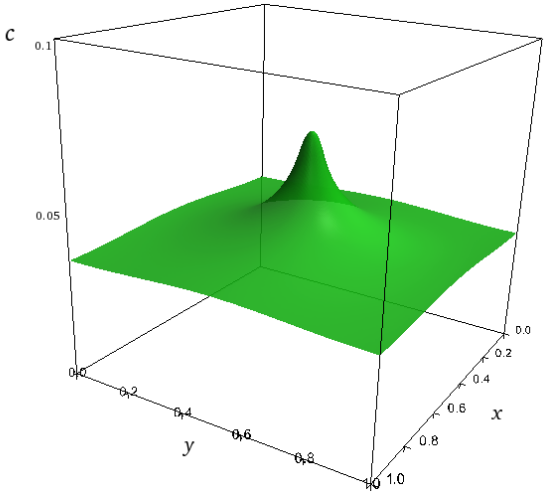

(b) $t = 49.020$.

After time $t > 150$, $c \to 0$ (equilibrium).

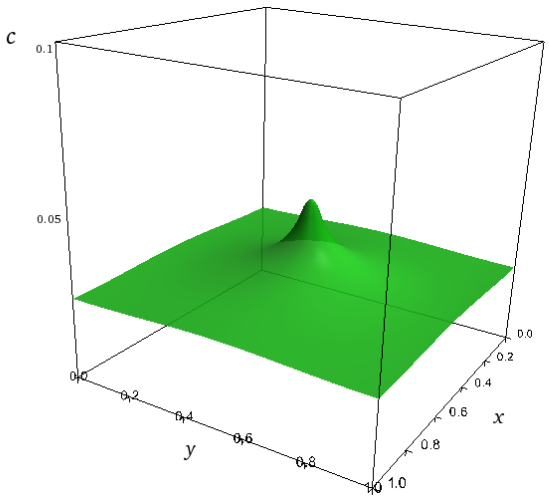

(c) $t = 88.235$.

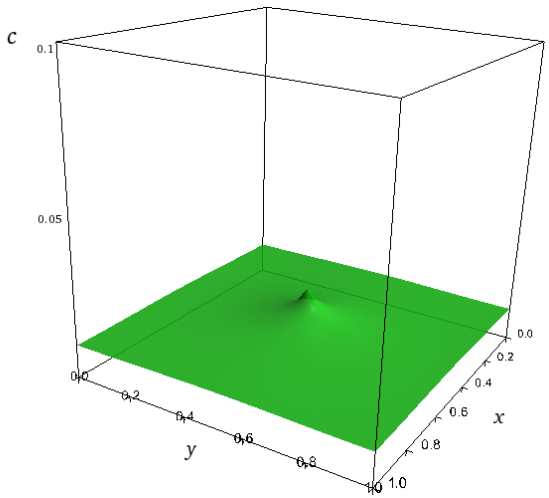

(d) $t = 147.159$.

Figure: Concentration c for small-diffusion of v. Metastable state forms after short times. They persist for large times. Eventually $c \to 0$ as $t \to +\infty$.

Concentration u (small-diffusion). Invasive front as in the zer-diffusion limit for short times.

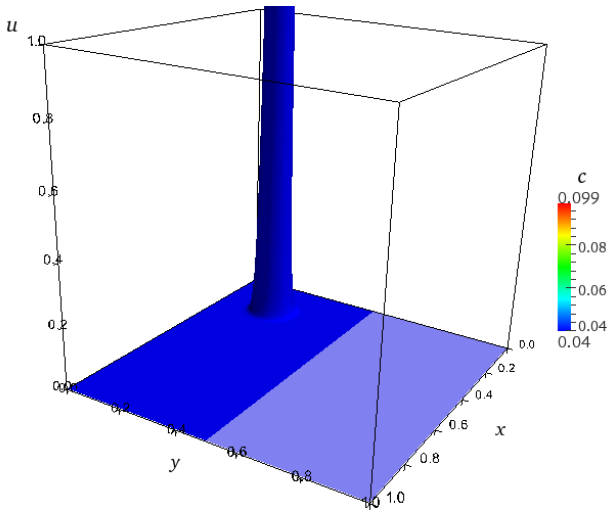

(a) $t = 0$.

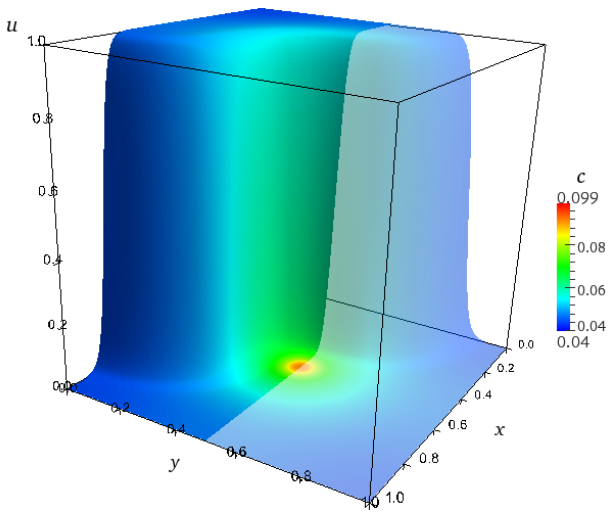

(b) $t = 1.961$.

Formation of an equilibrium matestable front at time $t > 6$.

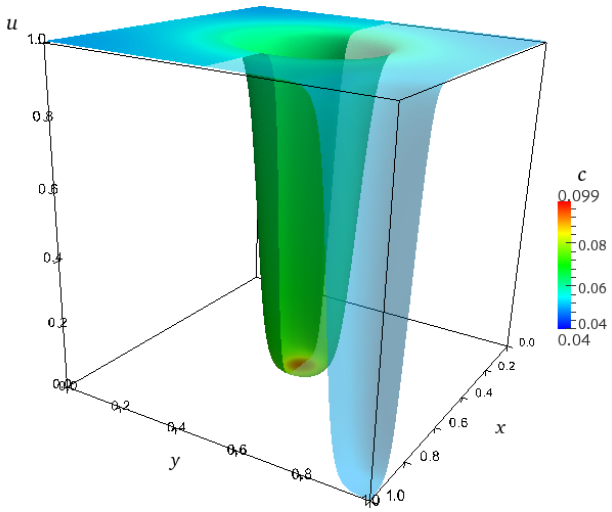

(c) $t = 4.902$.

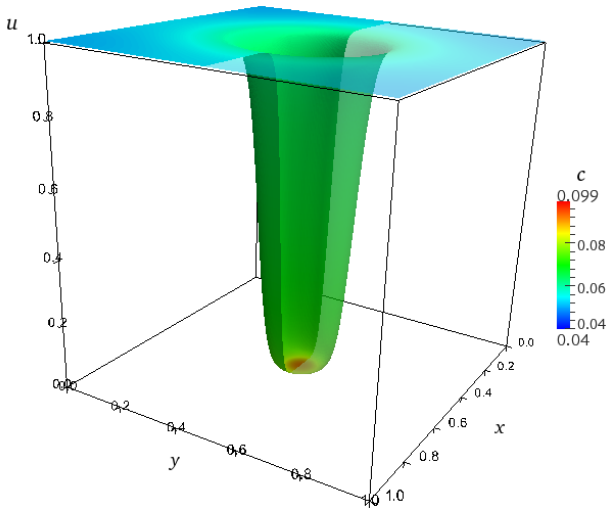

(d) $t = 5.882$.

Persistence of the transient front in u for large times.

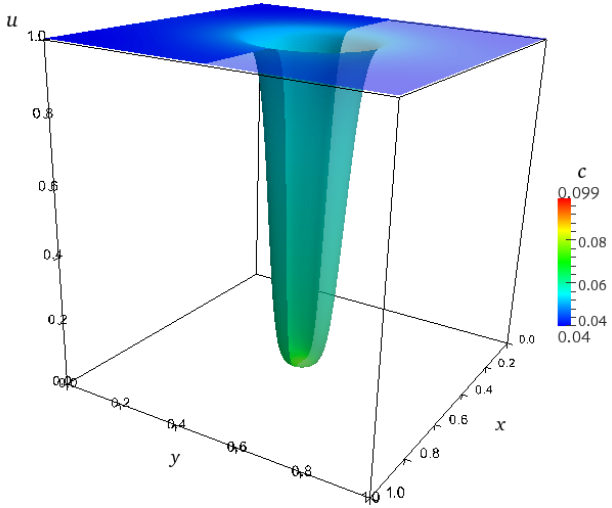

(e) $t = 50.$

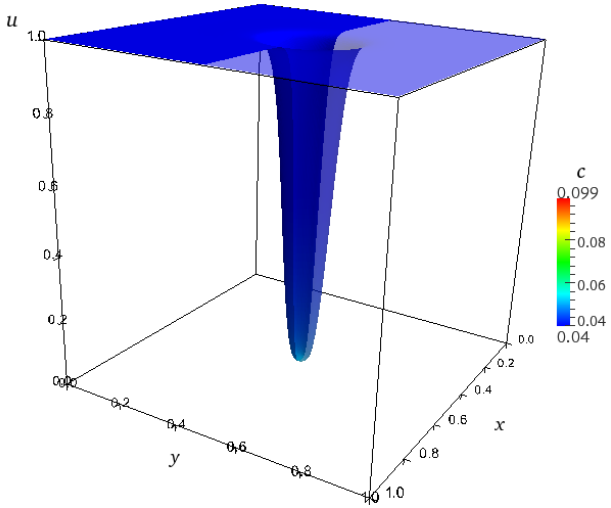

(f) $t = 99.020.$

Solution eventually reaches equilibrium constant solution (invasion). The time existence of the transient is larger if D_v is smaller.

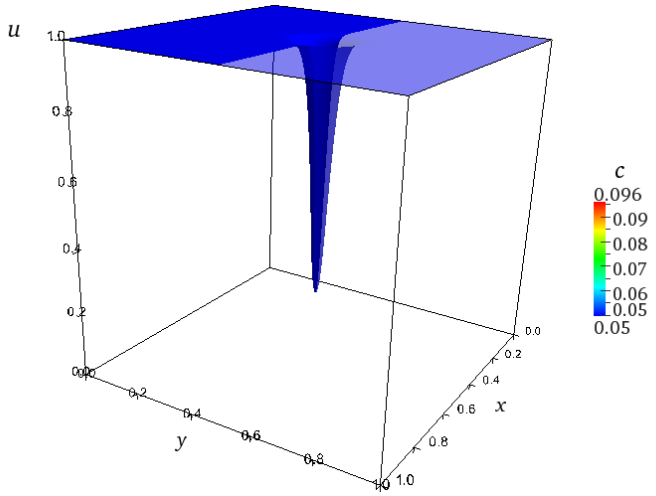

(g) $t = 147.059$.

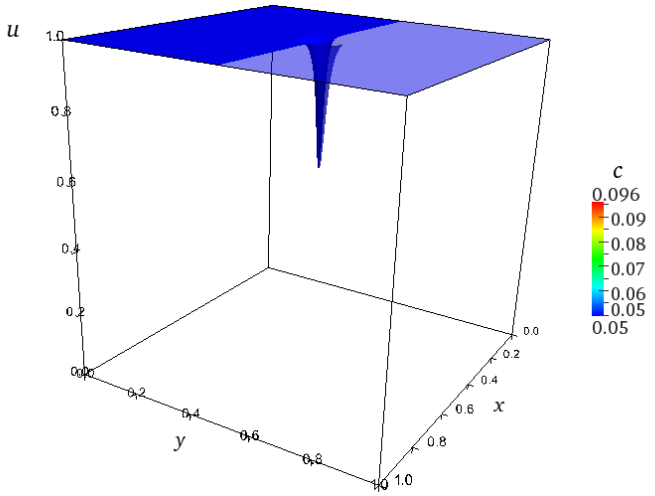

(h) $t = 166.667$.

Figure: Concentration u evolution for small-diffusion $D_v = 10^{-5}$. Transient equilibrium front eventually vanishes for large times.

Stationary states for $D_v = 0$ are good approximations of transient layers when $D_v \ll 1$.

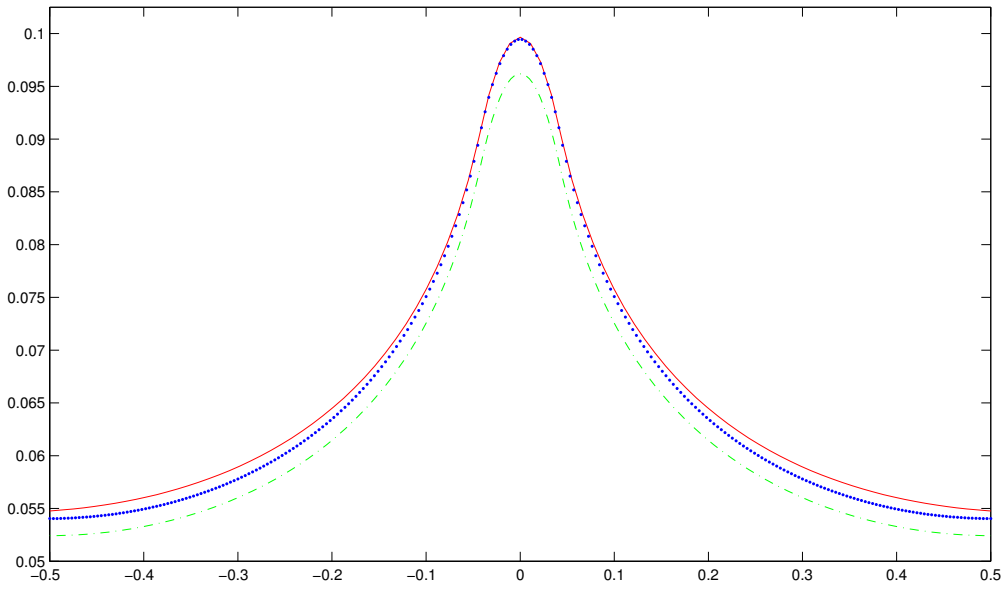

Figure: Cross section of concentration of c. Continuous (red) plot is the analytic solution for a circular domain when $D_v = 0$. Dotted blue graph is the numerical stationary solution for $D_v = 0$ at time $t = 9.8039$. Dashed (green) graph is the transient layer at time $t = 9.8039$ for $D_v = 10^{-5}$.

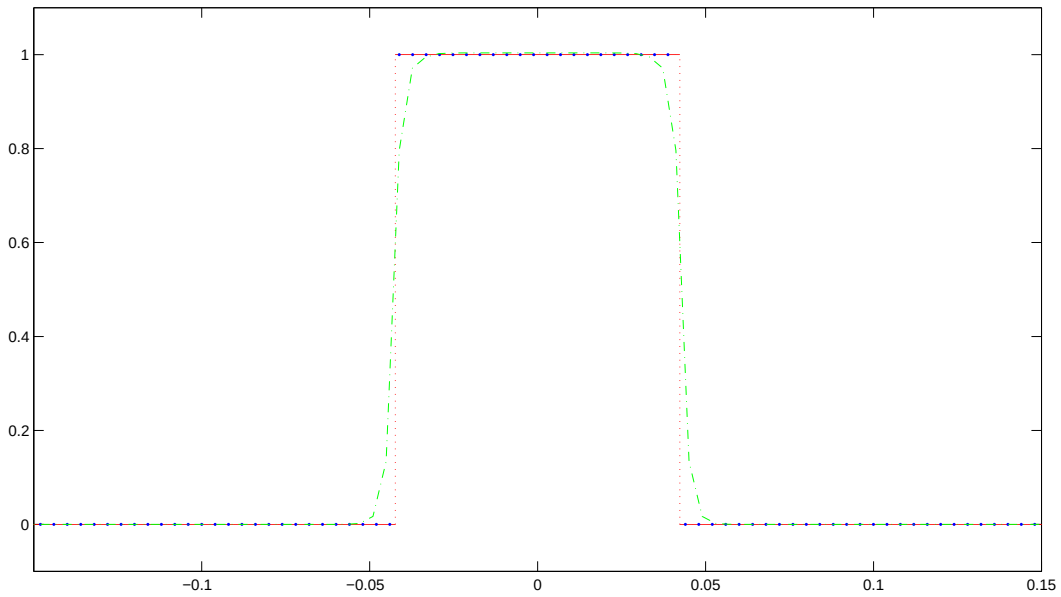

Figure: Cross section of concentration of v. Continuous (red) plot is the plateau for a circular domain when $D_v = 0$. Dotted blue graph is the numerical stationary solution when $D_v = 0$ at time $t = 9.8039$. Dashed (green) graph is the smooth transient layer at time $t = 9.8039$ for $D_v = 10^{-5}$.

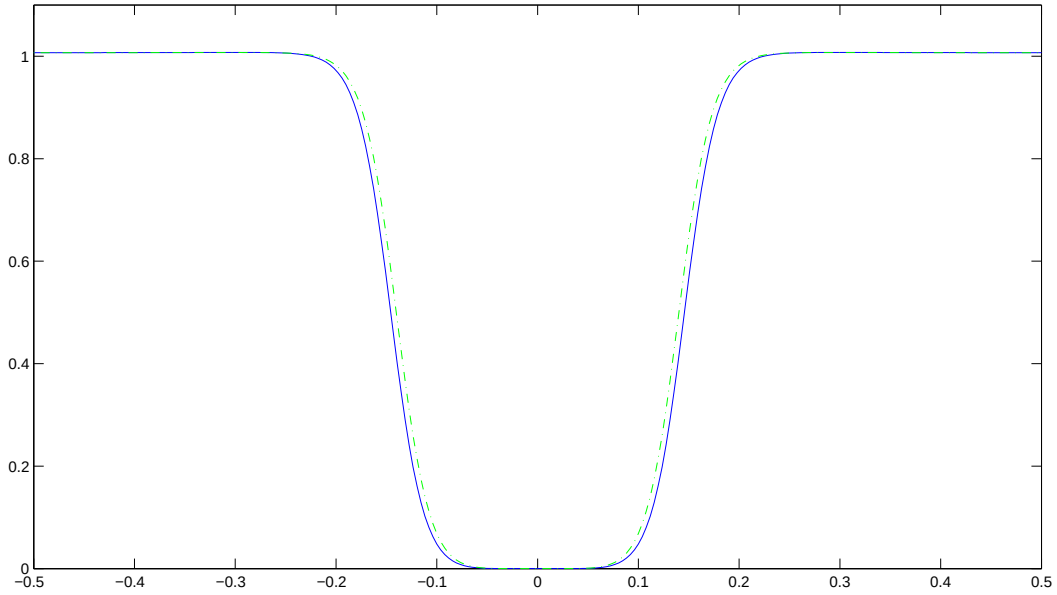

Figure: Cross section of concentration of u. Dotted blue graph is the numerical stationary circular front when $D_v = 0$ at time $t = 9.8039$. Dashed (green) graph is the transient (metastable) invasive front at time $t = 9.8039$ for $D_v = 10^{-5}$.

Simulation no. 3: the experiment of Swain and Ray

Initial condition for fungi (uniform concentration in the Petri dish - control):

$$u(x,y,0) = 0.21 > u_*,$$

Application of bacteria (two localized Gaussians):

$$v(x,y,0) = 3\left(e^{-1000((x-0.2)^2+(y-0.5)^2)} + e^{-1000((x-0.8)^2+(y-0.5)^2)}\right)$$

Initial chemical concentration: $c(x,y,0) = 0$.

Simulations for $D_v = 0$. Stationary solutions resemble transient layers observed in experiments.

Simulation no. 3: the experiment of Swain and Ray

Initial condition for fungi (uniform concentration in the Petri dish - control):

$$u(x,y,0) = 0.21 > u_*,$$

Application of bacteria (two localized Gaussians):

$$v(x,y,0) = 3\left(e^{-1000((x-0.2)^2+(y-0.5)^2)} + e^{-1000((x-0.8)^2+(y-0.5)^2)}\right)$$

Initial chemical concentration: $c(x,y,0) = 0$.

Simulations for $D_v = 0$. Stationary solutions resemble transient layers observed in experiments.

Simulation no. 3: the experiment of Swain and Ray

Initial condition for fungi (uniform concentration in the Petri dish - control):

$$u(x,y,0) = 0.21 > u_*,$$

Application of bacteria (two localized Gaussians):

$$v(x,y,0) = 3\left(e^{-1000((x-0.2)^2+(y-0.5)^2)} + e^{-1000((x-0.8)^2+(y-0.5)^2)}\right)$$

Initial chemical concentration: $c(x,y,0) = 0$.

Simulations for $D_v = 0$. Stationary solutions resemble transient layers observed in experiments.

Concentration of v. Formation of two steady localized plateau.

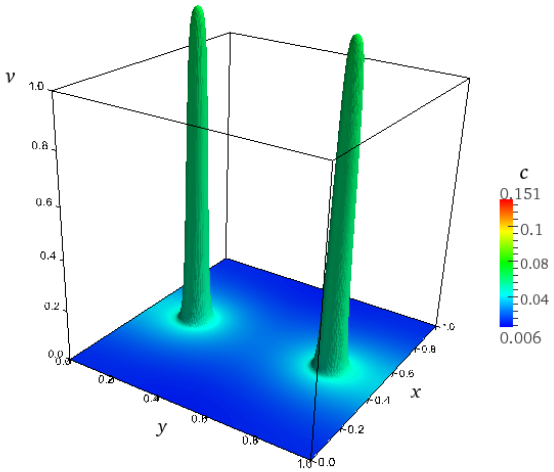

(a) $t = 0.1569$.

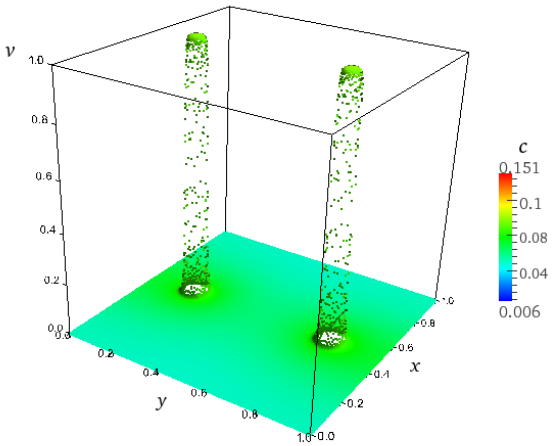

(b) $t = 0.5882$.

Stationary solution for v at time $t = 9.8039$.

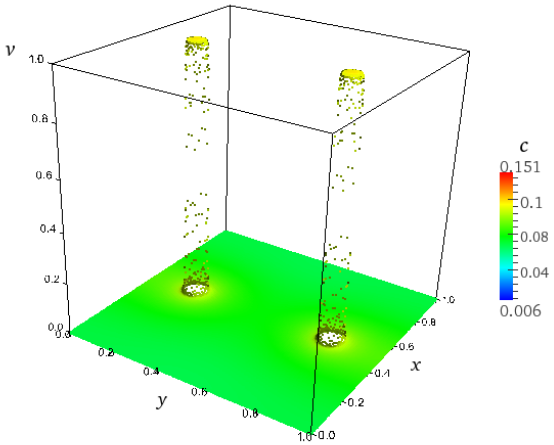

(c) $t = 0.9804$.

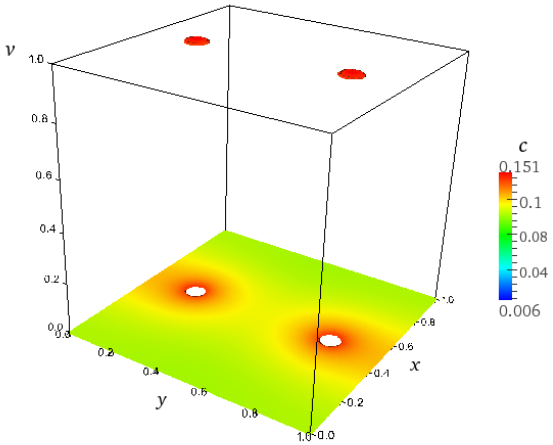

(d) $t = 9.8039$.

Figure: Concentration of v, in the $D_v = 0$ case. Formation of a stationary solution.

The v solution induces a steady solution for the chemical c.

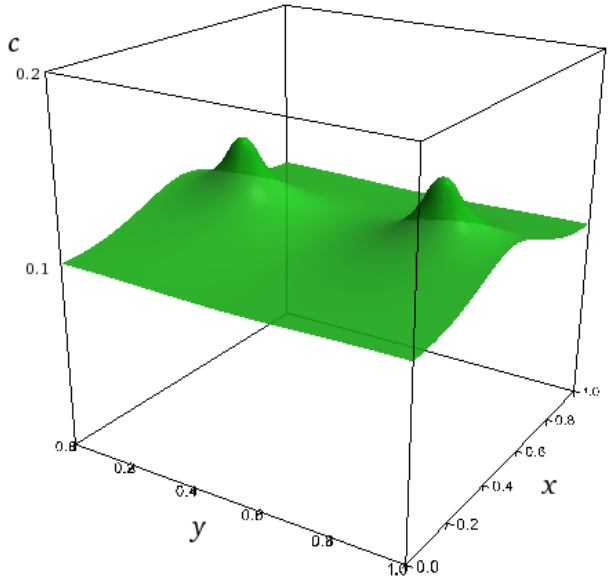

Figure: Chemical concentration c at time $t = 9.8039$.

Evolution of u. Uniform distribution at $t = 0$.

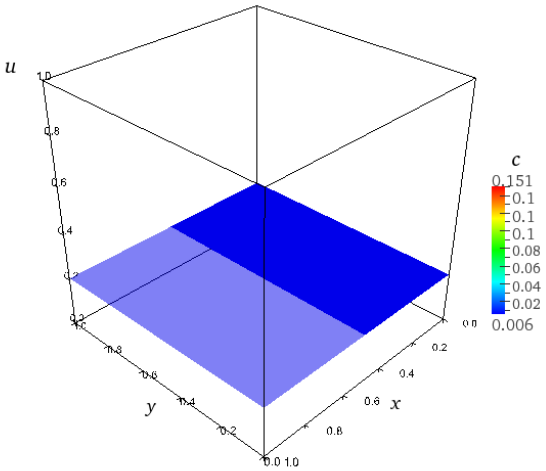

(a) $t = 0$.

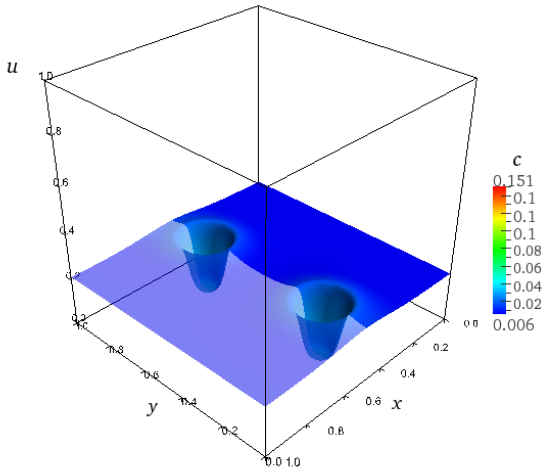

(b) $t = 0.0392$.

Invasive fronts meet the chemical gradient.

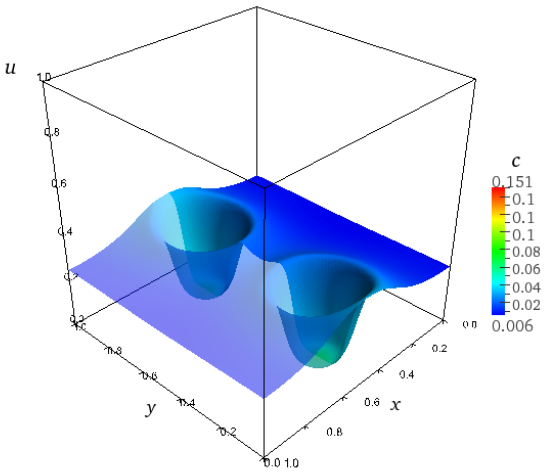

(c) $t = 0.1176.$

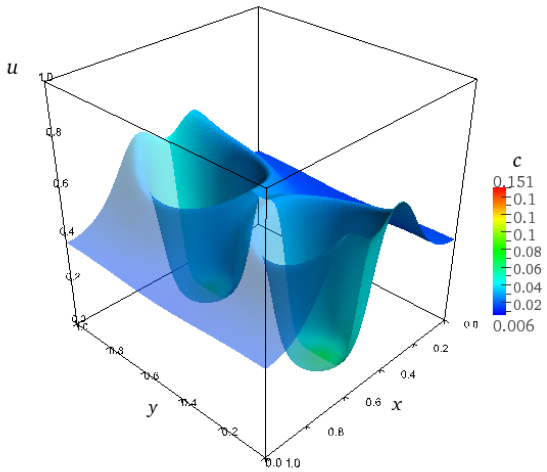

(d) $t = 0.1961.$

Superposition (to leading order) of two circular fronts.

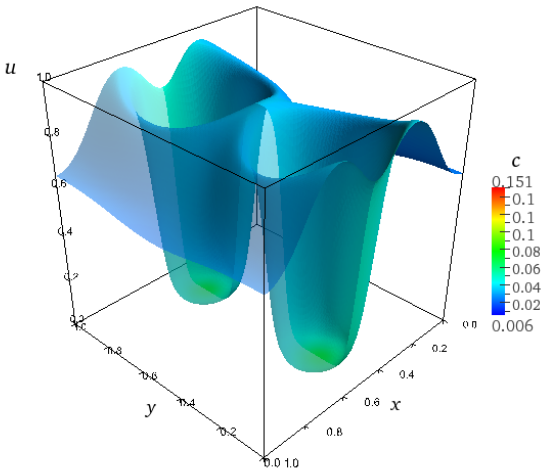

(e) $t = 0.2549.$

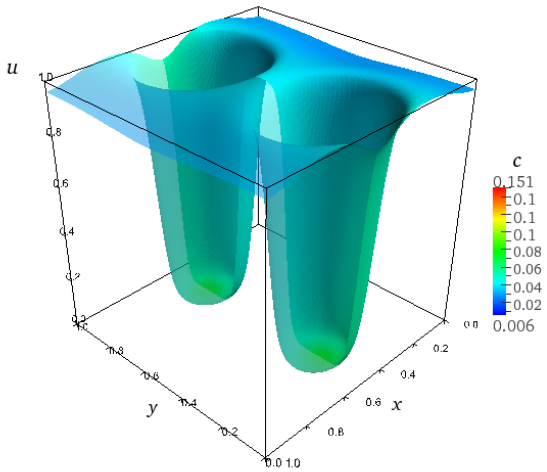

(f) $t = 0.3137.$

Stationary circular fronts (at equilibrium).

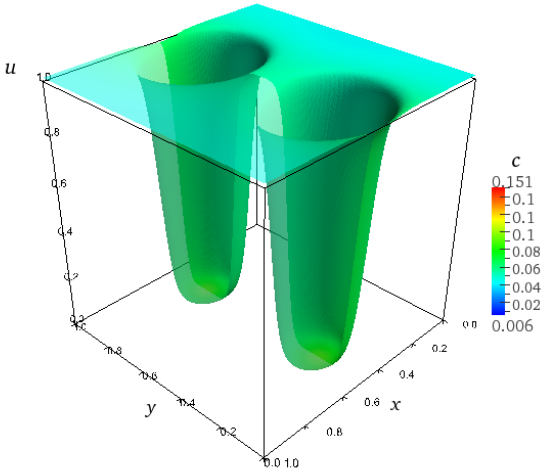

(g) $t = 0.4902$.

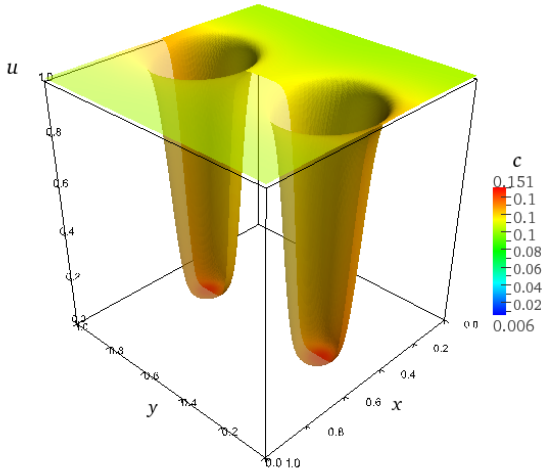

(h) $t = 9.8039$.

Figure: Evolution of u. Two invasive fronts reach equilibrium.

Top view of the circular steady fronts.

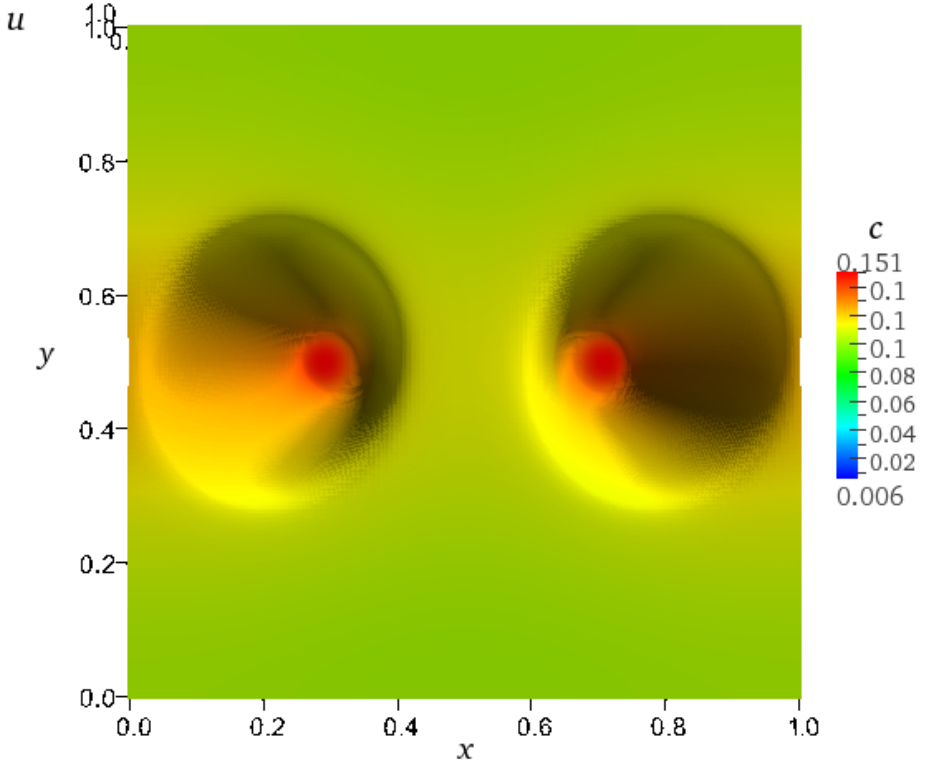

Conclusions

- Simplest model for inhibition of an invading front, triggered by the chemical produced by another species (basic negative chemotactic mechanism)
- Cell colonies small diffusivity regime
- Basic state: for a circular domain there are radially symmetric steady states (in the zero-diffusion limit for one of the species)
- Repulsion by the chemical gradient of an invading front
- Stable in the front propagation limit

- Approximates well the numerically computed steady front in a square domain
- In the small-diffusivity regime: emergence of metastable/transient patterns, well-approximated by the steady states
- Fungus pattern from experimental results shows the same qualitative dynamics (superposition of the basic states)

Thank you!